

## Supporting Information

# Polar Organic Cages for Efficient Azeotropic Mixtures Separation

Lukman O. Alimi,<sup>a</sup> Xin Liu,<sup>a</sup> Gengwu Zhang,<sup>a</sup> Basem Moosa<sup>a</sup> and Niveen M. Khashab<sup>a\*</sup>

<sup>a</sup> Smart Hybrid Materials (SHMs) Laboratory, Physical Science and Engineering, King Abdullah University of Science and Technology (KAUST), Thuwal 23955-6900, Kingdom of Saudi Arabia.

### Materials and Methods

All reagents were commercially available and used as supplied without further purification. Compound **DIHO-cage** was synthesized by modifying the previous literature report.<sup>1</sup>

### Single Crystal Growth.

Single crystals of **DIHO-cage@DCM** and **DIHO-cage@CHCl<sub>3</sub>** were obtained by vapor diffusion of acetonitrile into DCM and chloroform solution of **DIHO-cage** at room temperature respectively; Colourless and suitable single crystals of **DIHO-cage@Tol** and **DIHO-cage@Py** were also obtained after 3 days by vapor diffusion of acetonitrile into **DCM/Tol** and **DCM/Py** solutions of **DIHO-cage** at room temperature respectively.

### Single X-ray Crystal Structure Determination

Single crystal X-ray diffraction data were recorded on a Bruker D8 Venture and Metaljet equipped with a digital camera diffractometer using graphite-monochromated CuK $\alpha$  radiation ( $\lambda = 1.5418$  Å) and GaK $\alpha$  radiation ( $\lambda = 1.34139$  Å) respectively for the crystal structures. Data reductions were carried out by means of a standard procedure using the Bruker software package SaintPlus 6.01.<sup>2</sup> The absorption corrections and the correction of other systematic errors were performed using SADABS.<sup>3</sup> The structures were solved by direct methods using SHELXS-2008 and refined using SHELXL-2018.<sup>4</sup> X-Seed<sup>5</sup> and OLEX2<sup>6</sup> were used as the graphical interface for the SHELX program suite. Anisotropic thermal parameters were applied to all non-hydrogen atoms. All the

hydrogen atoms were generated geometrically. Data collection, structure refinement parameters and crystallographic data for the crystals are given in Table S1.

### **Activation of DIHO-cage.**

Crystalline **DIHO-cage** materials were activated under vacuum at 40 °C for 2 h to obtain the activated **DIHO-cage**. While the activated **DIHO-cage** after adsorption of **Tol** was regenerated by releasing the adsorbed guests upon heating at 70 °C under vacuum for 3 h. Alternatively, the **DIHO-cage** was also regenerated after adsorption by first washing with *n*-hexane and then activated at much lower temperature of 45 °C under vacuum for 1 h.

### **Solid-vapor Adsorption Experiments.**

An open 5 mL vial containing 10 mg of activated **DIHO-cage** was placed in a 20 mL vial containing 1 mL of each solvent and an equal volume 1:1 (v/v) binary mixture of **Tol/Py**. We also investigated the adsorption of **Tol** at much lower ratio of 1:3 (v/v) binary mixture of **Tol/Py**.

### **NMR**

NMR spectra were recorded on Bruker-400 (400 MHz for <sup>1</sup>H; 101 MHz for <sup>13</sup>C) instruments internally referenced to SiMe<sub>4</sub> signal.

### **PXRD**

Powder X-ray diffraction (PXRD) patterns were obtained using a XRD Bruker D8-ADVANCE X-ray diffractometer (40 KV, 40 mA) with the Cu K $\alpha$  radiation ( $\lambda = 1.5418 \text{ \AA}$ ). Data were measured over the range of 3.5–40° in 2°/min steps. The sample was placed in a zero-background sample holder and normal configuration of the instrument was used.

### **GC-MS**

Gas chromatography (GC) analysis. GC measurements were carried out using an Agilent 7890A instrument configured with an FID detector and a DB-VRX column (60 m  $\times$  0.250 mm  $\times$  0.14  $\mu$ m). The following GC method was used: the oven was programmed from 70 °C, and ramped in 10 °C min<sup>-1</sup> increments to 150 °C with 15 min hold; the total run time was 25 min; injection

temperature was 250 °C; detector temperature was 250 °C with hydrogen, air, and make-up flow-rates of 40, 400, and 15 mL min<sup>-1</sup>, respectively; helium (carrier gas) flowrate was 3.0 mL min<sup>-1</sup>.

## TGA

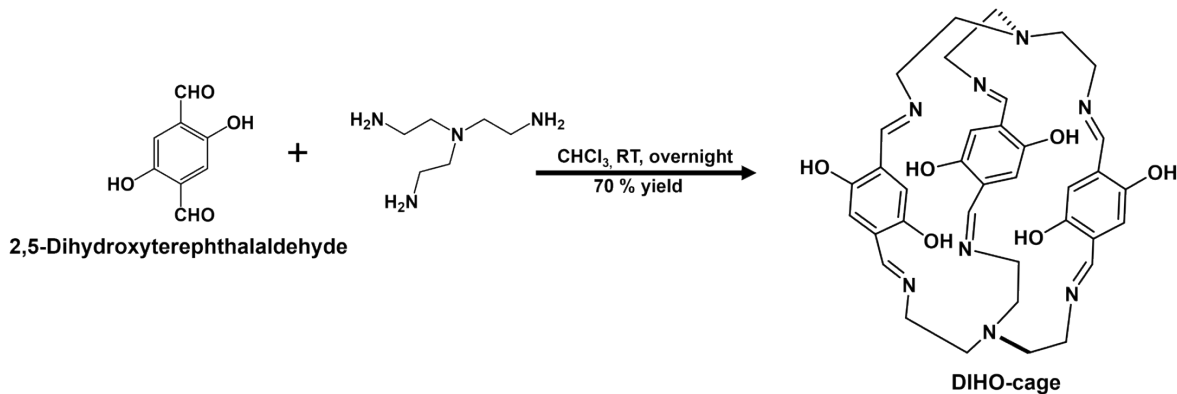
Thermogravimetric analysis was carried out using an automatic sample loading TA Instruments Q50 analyzer. The samples were heated starting at room temperature to 700 °C using nitrogen as the protective gas.

## BET Analysis

Low-pressure gas adsorption measurements were performed on a Micromeritics Accelerated Surface Area and Porosimetry System (ASAP) 2020 surface area analyzer. Sample was degassed under dynamic vacuum for 5 h at 40 °C prior to each measurement. N<sub>2</sub> isotherm was measured using a liquid nitrogen bath (77 K). CO<sub>2</sub> isotherm was also measured at 196 K.

## Synthesis of DIHO-cage

Tris(2-aminoethyl) amine (Tren) (292.48 mg; 2.0 mmol) was dissolved in MeCN (5 mL) and was added dropwise over 1 h to the solution of 2,5-Dihydroxyterephthalaldehyde (498.39 mg; 3.0 mmol) in MeCN (50 mL). The reaction mixture was stirred overnight at room temperature. A light-yellow precipitate was formed which was filtered and washed further with MeCN, then dissolved in dichloromethane and filtered to remove polymers. After the removal of dichloromethane, **DIHO-cage** was obtained in 70% yield.



**Scheme S1:** Synthesis of **DIHO-cage**.

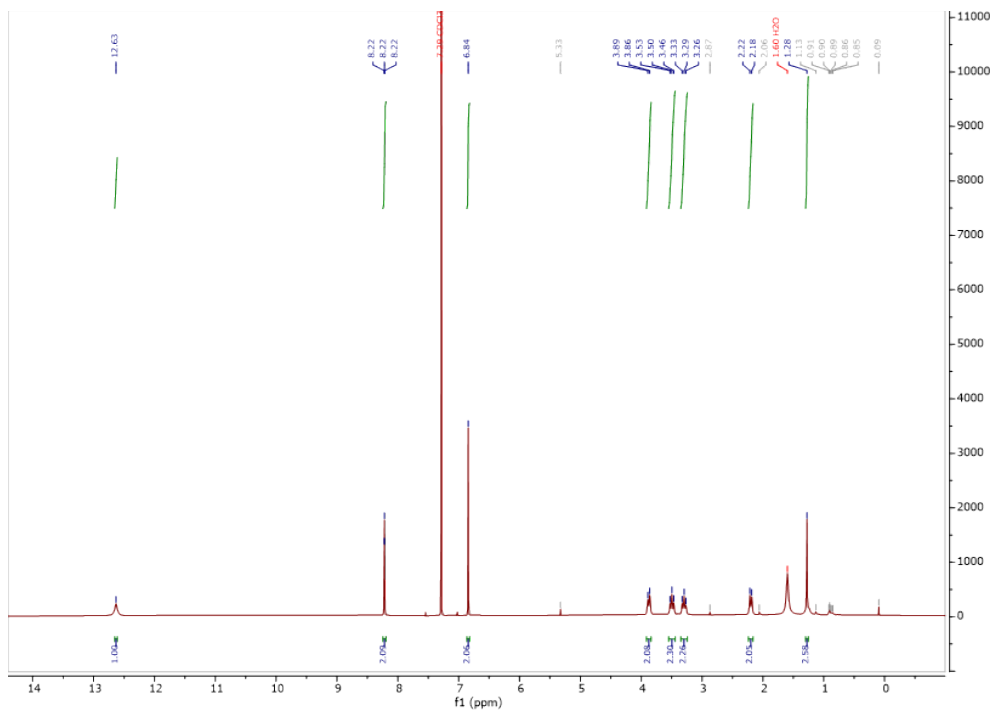


**Figure S1a:**  $^1\text{H}$  NMR spectrum (400 MHz,  $\text{CDCl}_3$ , 293 K) of the **DIHO-cage**.

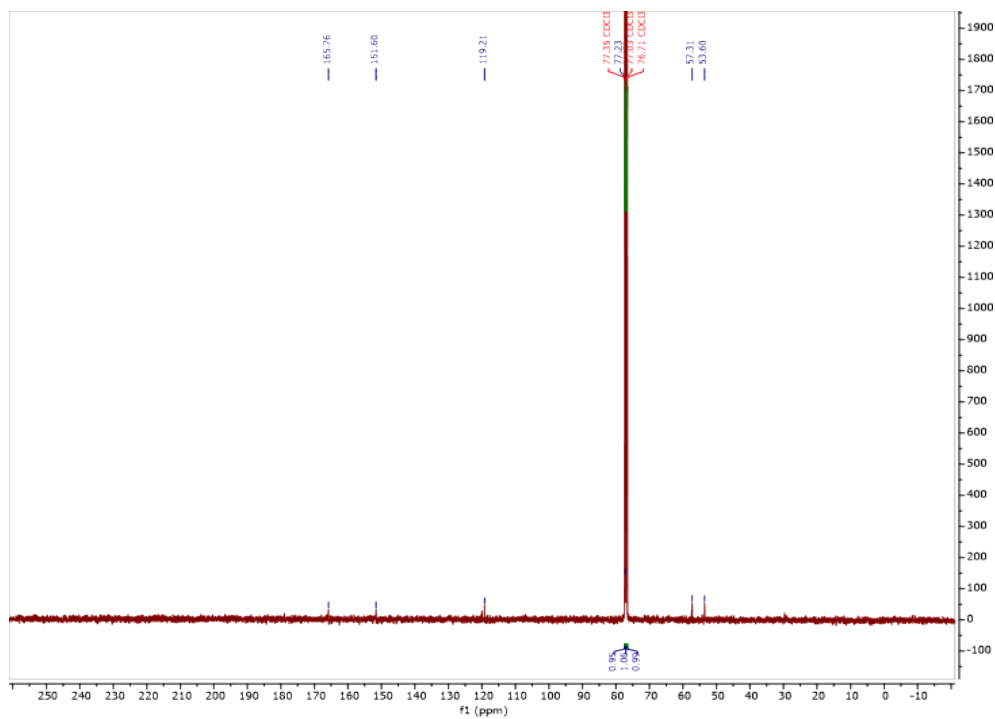


**Figure S1b:**  $^{13}\text{C}$  NMR spectrum (101 MHz, 298K,  $\text{CDCl}_3$ ) of the **DIHO-cage**.

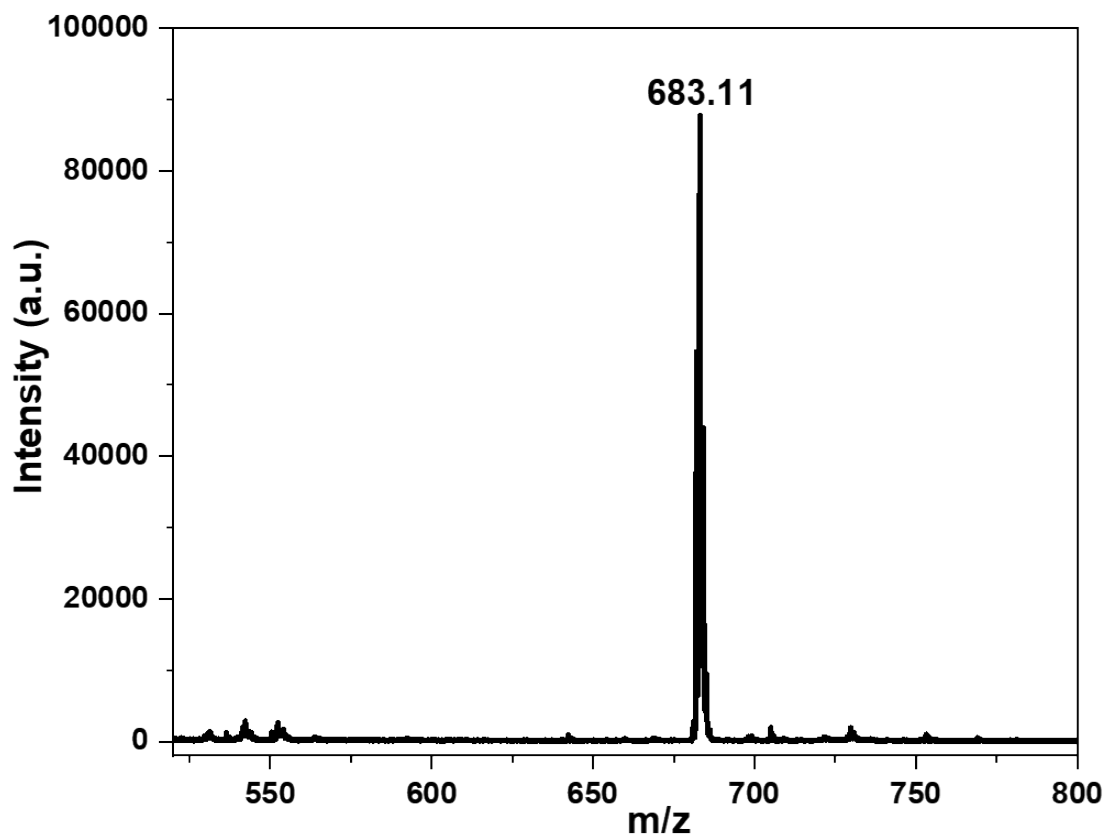


Figure S2: ESI-Mass spectrum of the DIHO-cage.

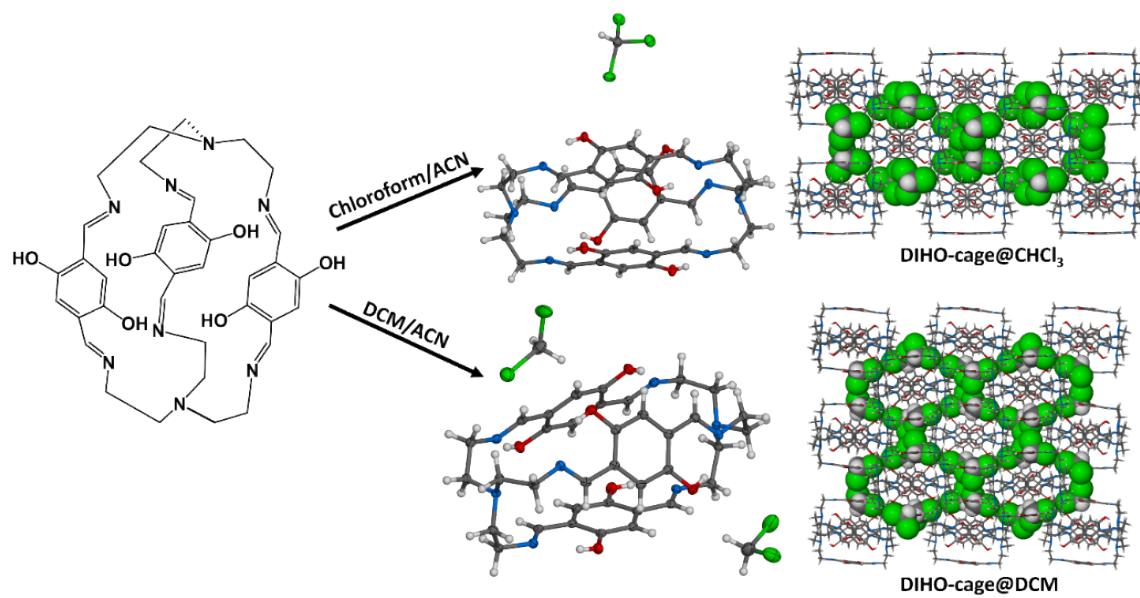
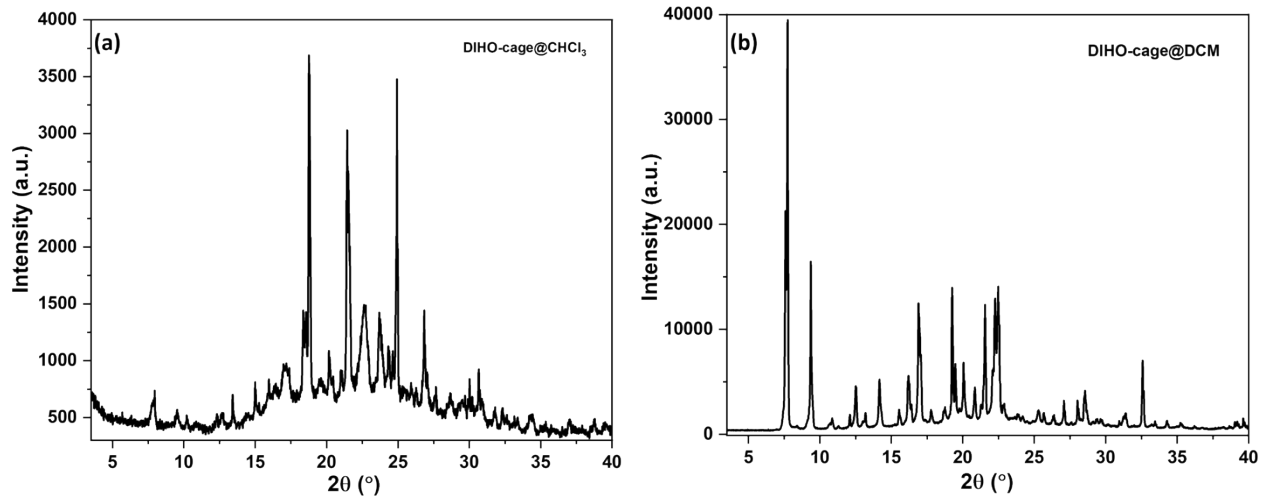
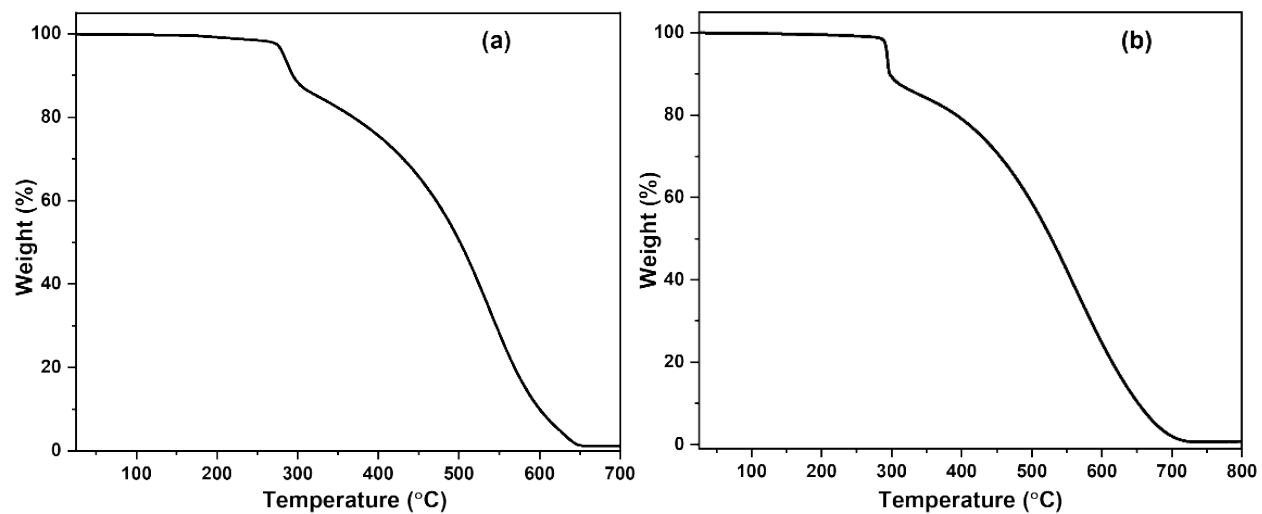


Figure S3a: Crystallization of DIHO-cage in Chloroform (DIHO-cage@CHCl<sub>3</sub>) and DCM (DIHO-cage@DCM).



**Figure S3b:** PXRD patterns of **DIHO-cage** in (a) Chloroform (**DIHO-cage@CHCl<sub>3</sub>**) and (b) DCM (**DIHO-cage@DCM**).



**Figure S4:** TGA curves of (a) assynthesized and (b) fully activated **DIHO-cage**.

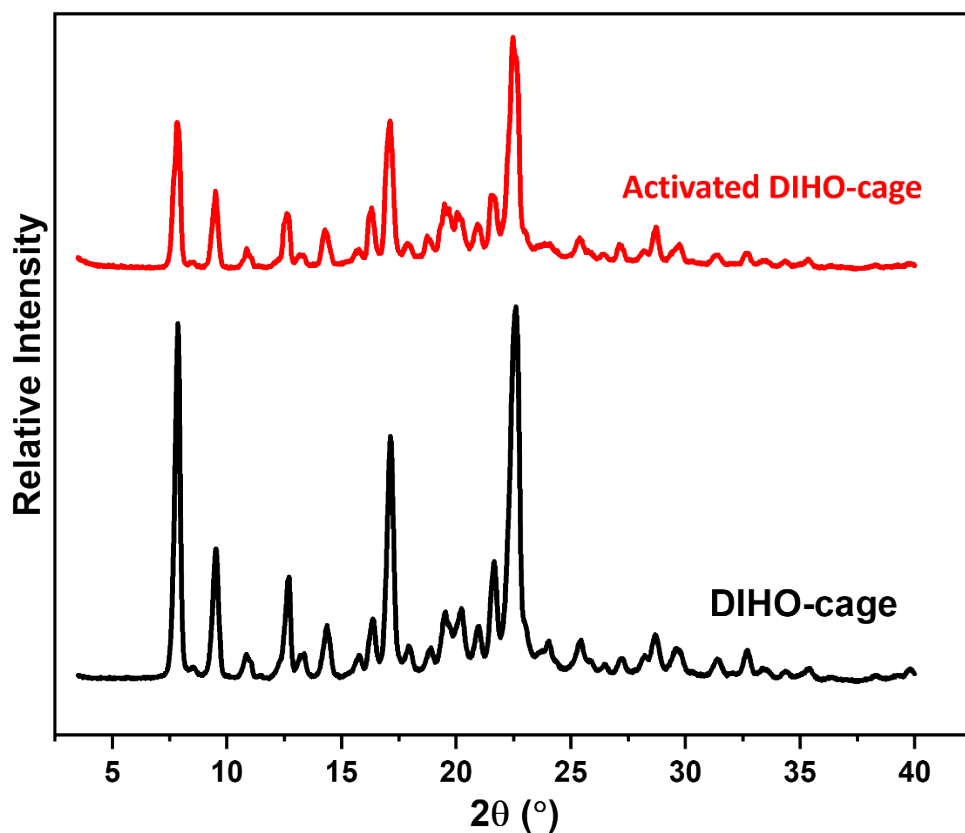


Figure S5: PXRD patterns of the assynthesized and activated DIHO-cage.

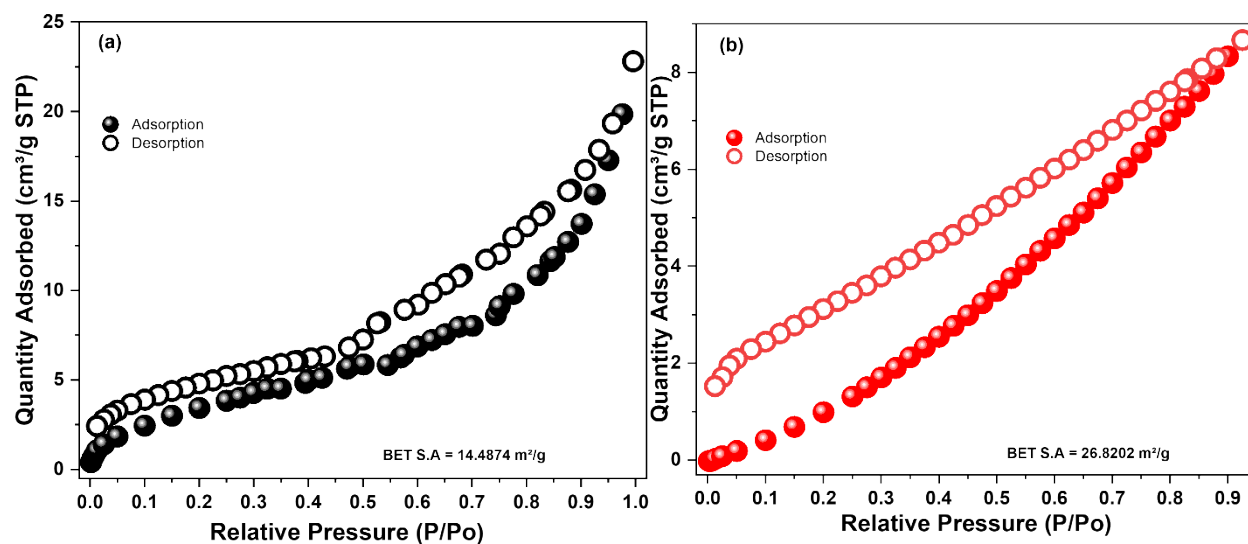
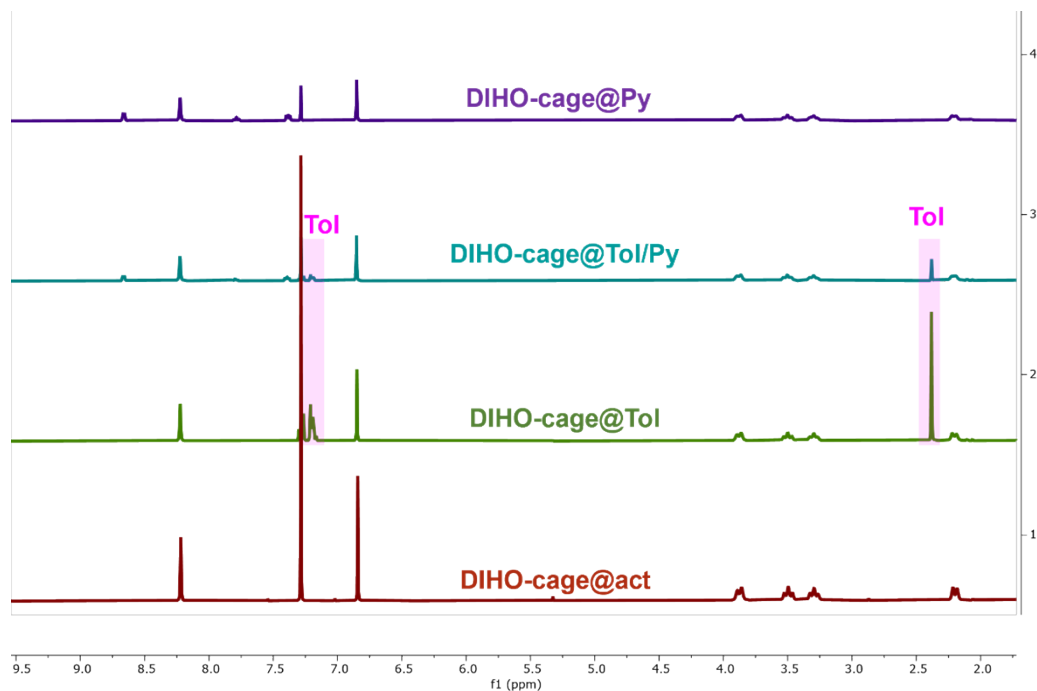
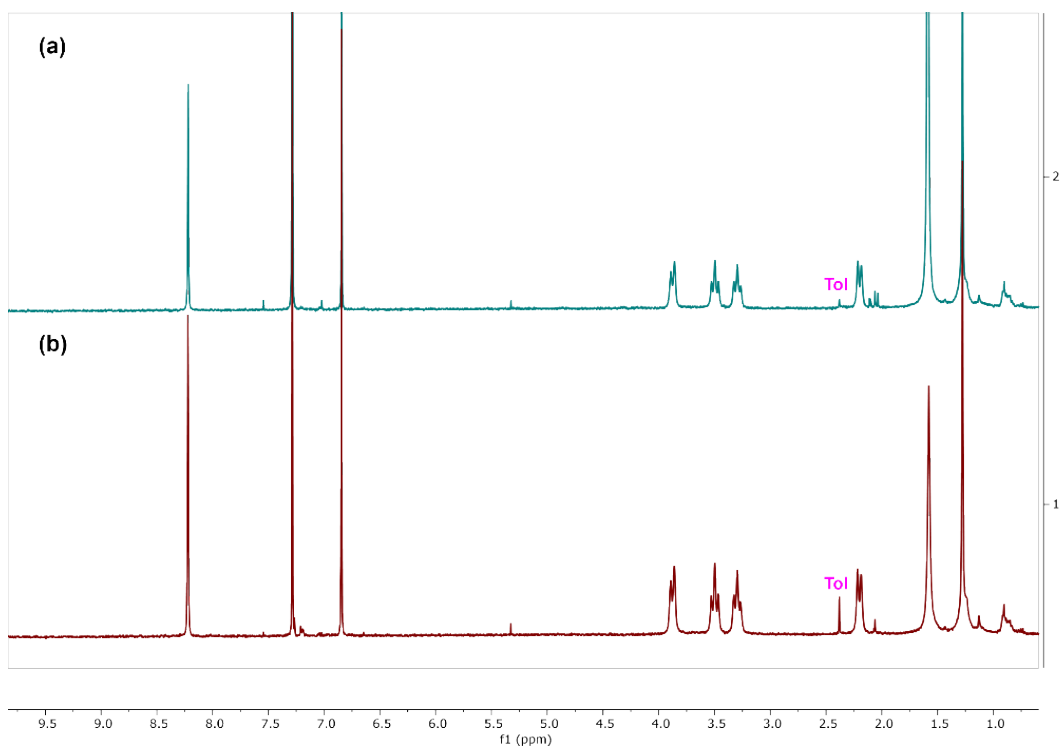


Figure S6: (a) Nitrogen gas sorption isotherm at 77 K and (b) CO<sub>2</sub> gas isotherm at 196 K for activated DIHO-cage.



**Figure S7:**  $^1\text{H-NMR}$  spectra (400 MHz,  $\text{CDCl}_3$ , 293 K) showing the adsorption of **Tol** and **Py** by activated DIHO-cage after 24 h exposure.



**Figure S8:** Magnified  $^1\text{H-NMR}$  spectra showing the uptake of **Tol** from **Tol/Py** (a) 1:3 (v/v) and (b) 3:1(v/v) binary mixture by activated DIHO-cage after 24 h.



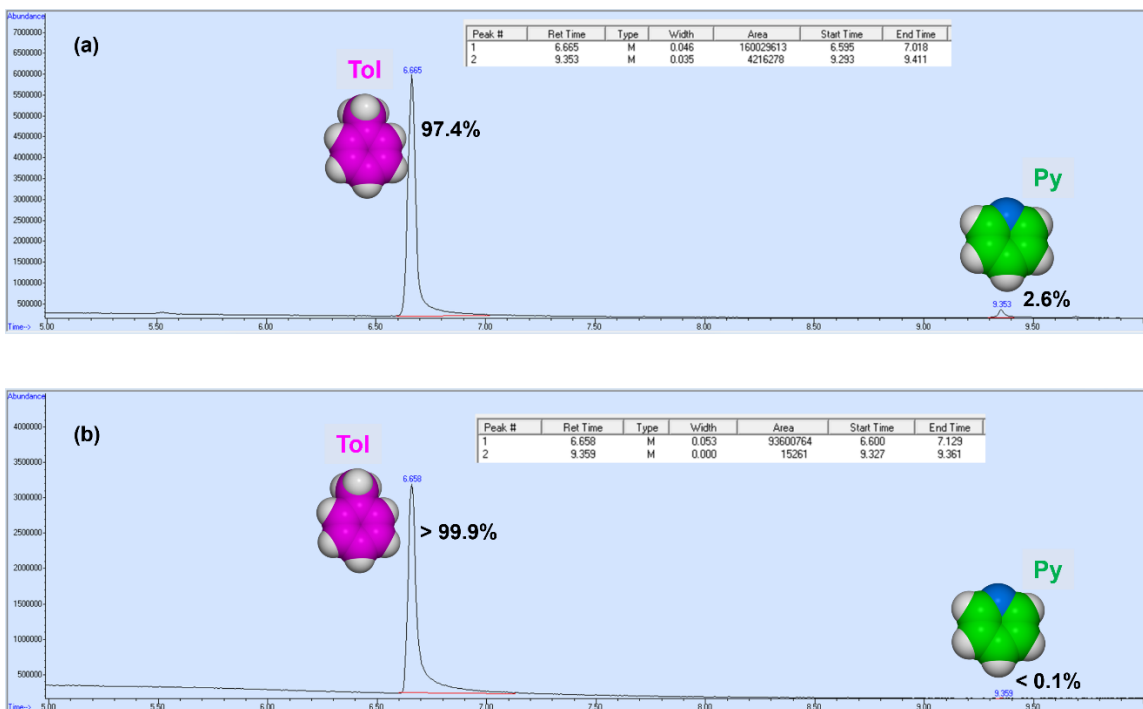


**Figure S9:** Relative amount of Tol and Py adsorbed from (a) 1:3 (v/v) and (b) 3:1 (v/v) Tol/Py mixtures by activated DIHO-cage as determined by gas chromatography.

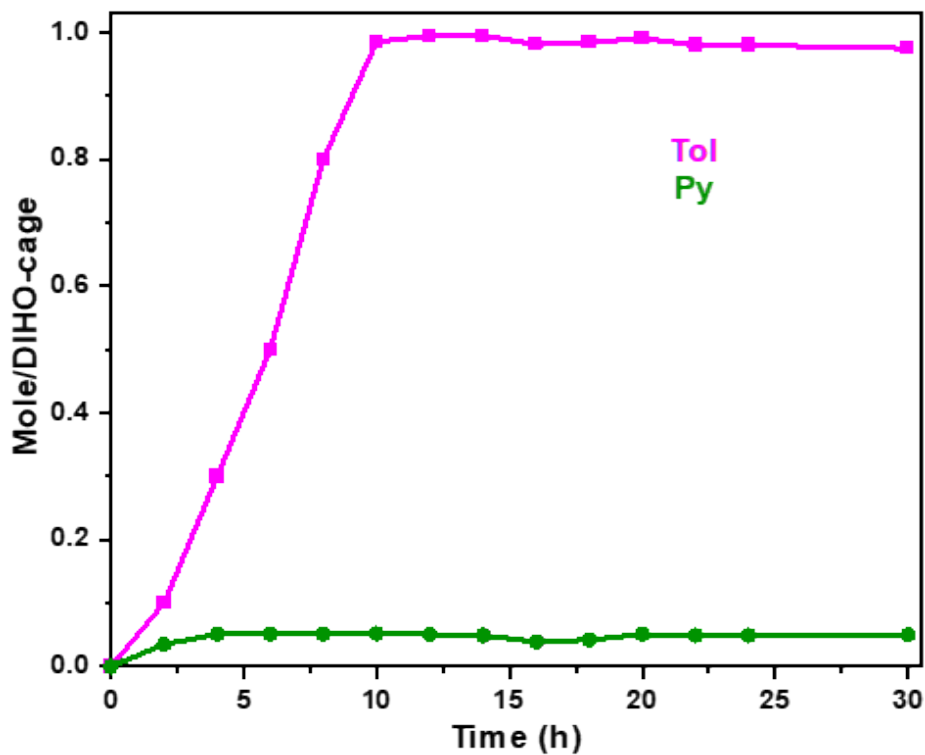


**Figure S10:** Time-dependent solid-vapor sorption plot for the 1:1 (v/v) of Tol/Py mixture by activated DIHO-cage.

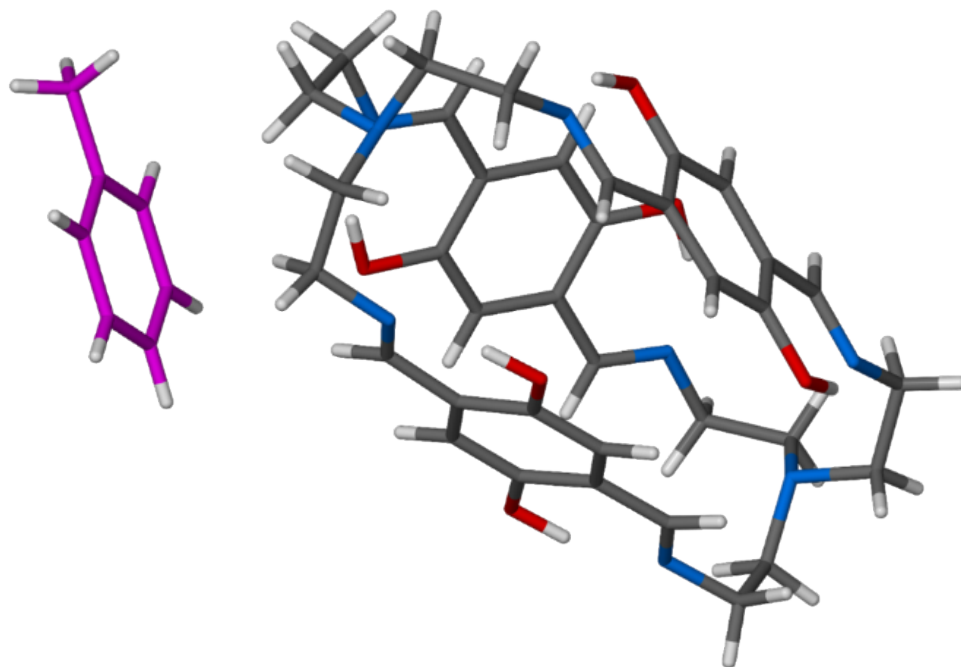


**Figure S11:** Asymmetric unit of the Crystal structure of **DIHO-cage@Tol** showing 1:1 host/guest ratio.

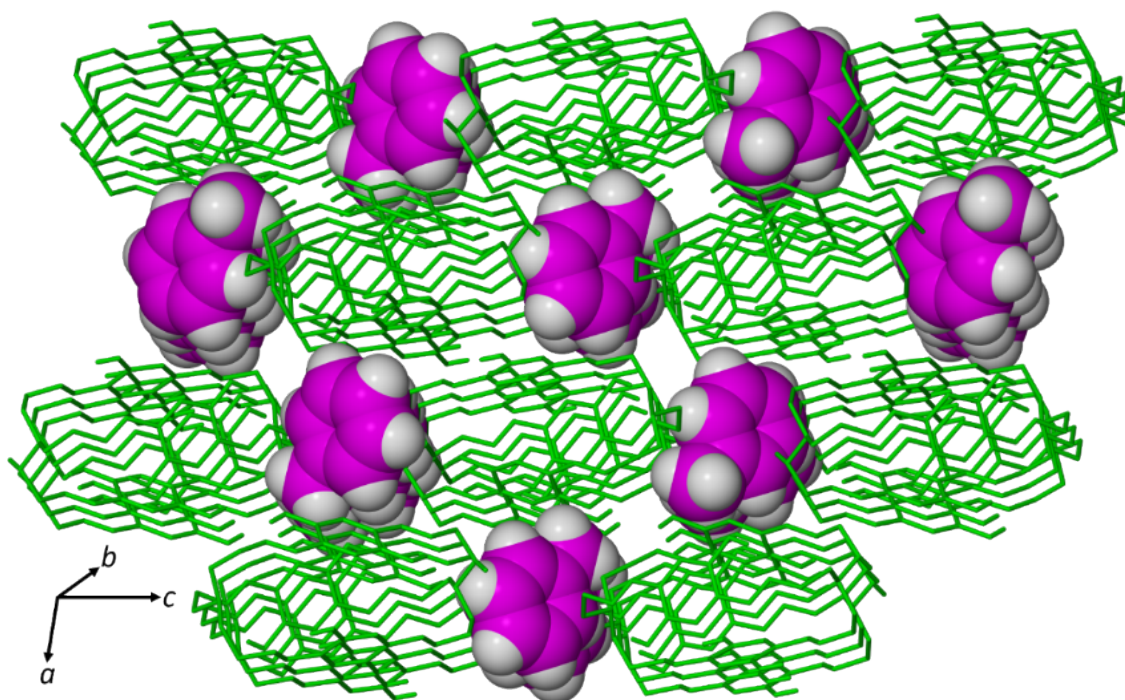


**Figure S12a:** Perspective view showing **Tol** (pink) in the channel of the crystal packing of **DIHO-cage@Tol** when viewed along *b*-axis.

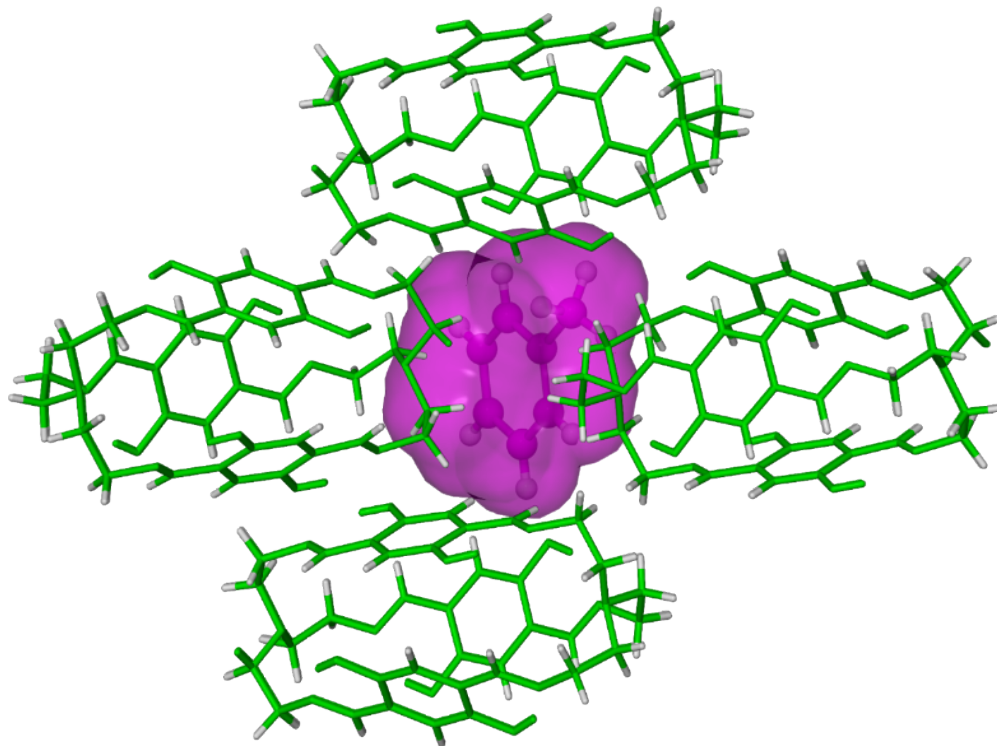


**Figure S12b:** Crystal packing showing the Tol guest (pink) occupied void using MSRoll program<sup>7</sup> when viewed along the crystallographic *b*-axis.

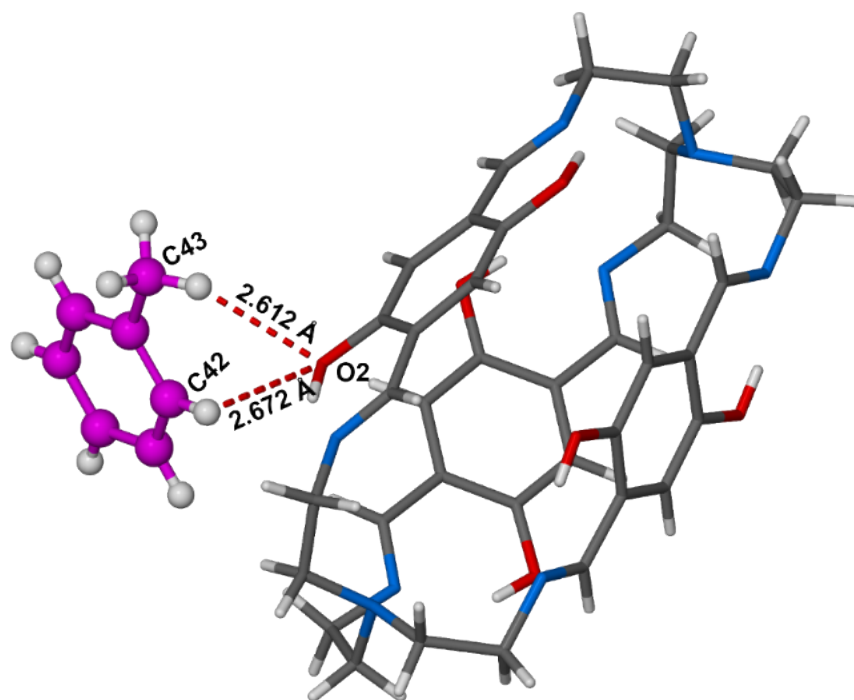


**Figure S13:** Crystal structure showing the C-H...O host-guest intermolecular interactions between DIHO-cage and Tol in DIHO-cage@Tol when viewed along *a*-axis.

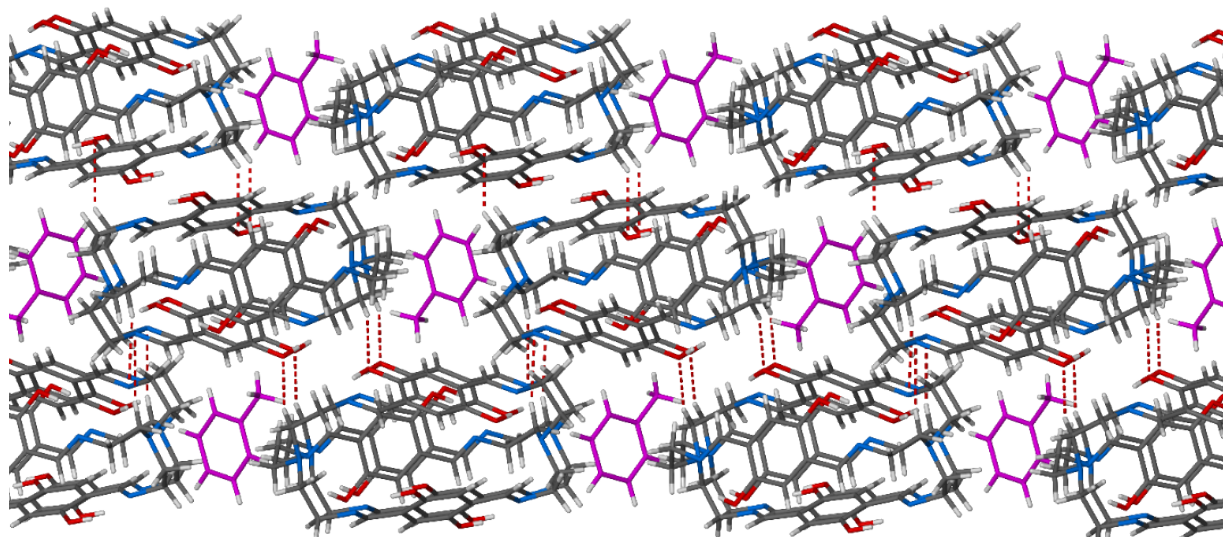


**Figure S14:** Perspective view showing C-H...O and C-H...N intermolecular hydrogen bonding interactions between the cages in **DIHO-cage@Tol** crystal structure.

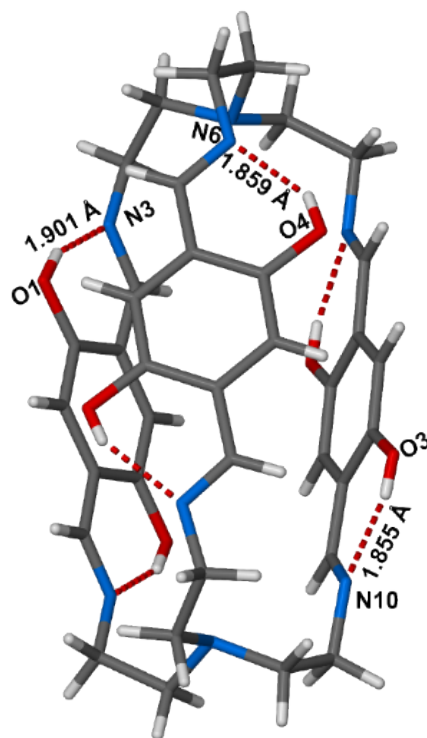


**Figure S15:** Perspective view showing very strong O-H...N intramolecular hydrogen bonding interactions within the cage in **DIHO-cage@Tol** crystal structure.

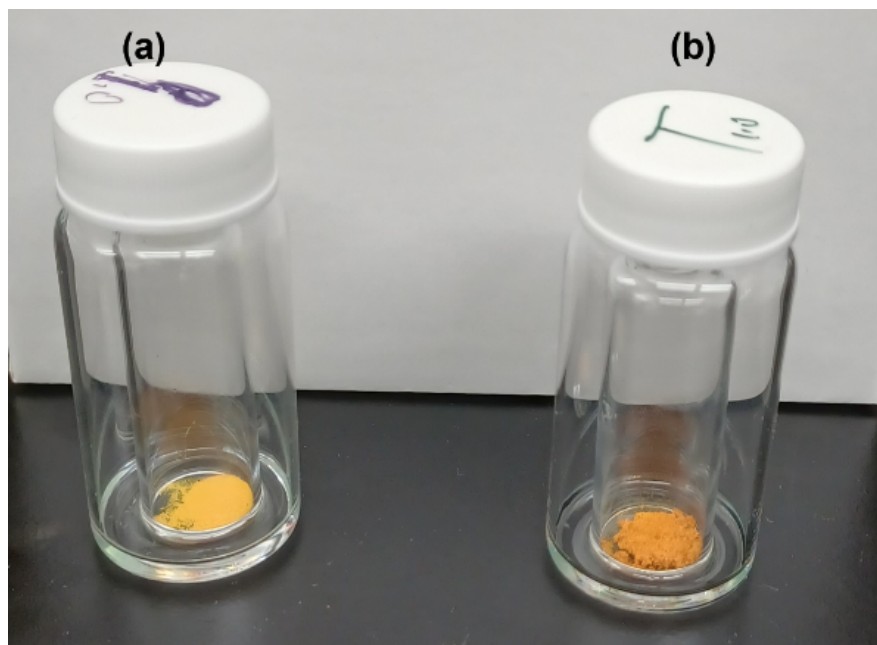


**Figure S16:** Images of solid-vapor adsorption of (a) pyridine and (b) toluene by the DIHO-cage after 24 h showing a vapo-chromic behaviour.

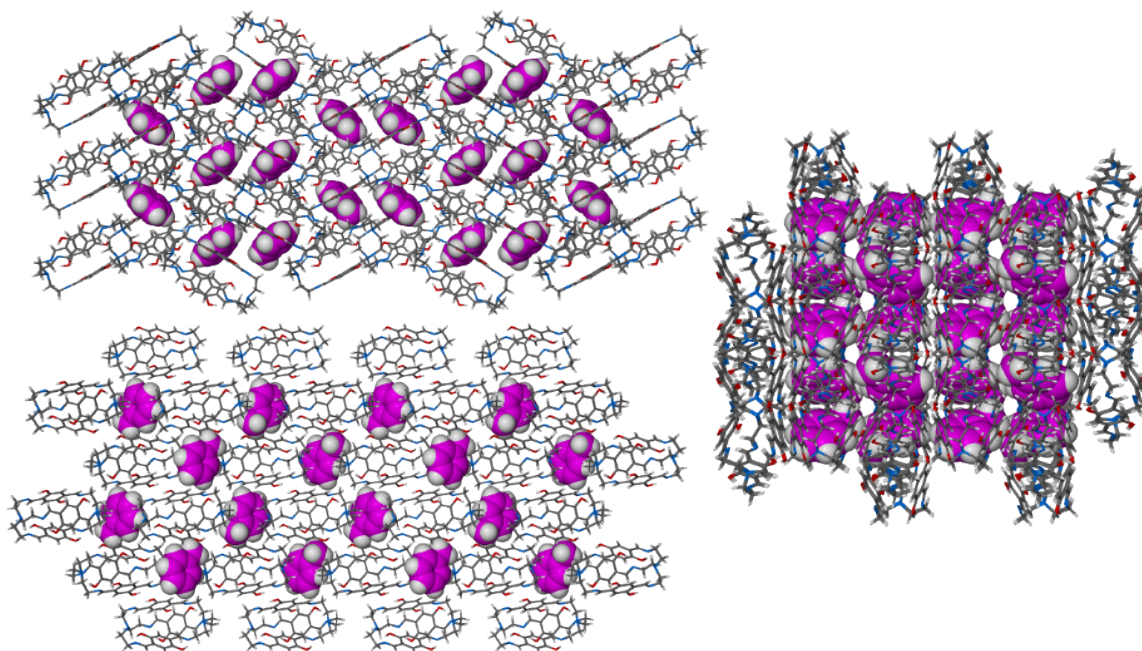


**Figure S17:** Crystal packing of DIHO-cage@Tol when viewed along all the three crystallographic axes.

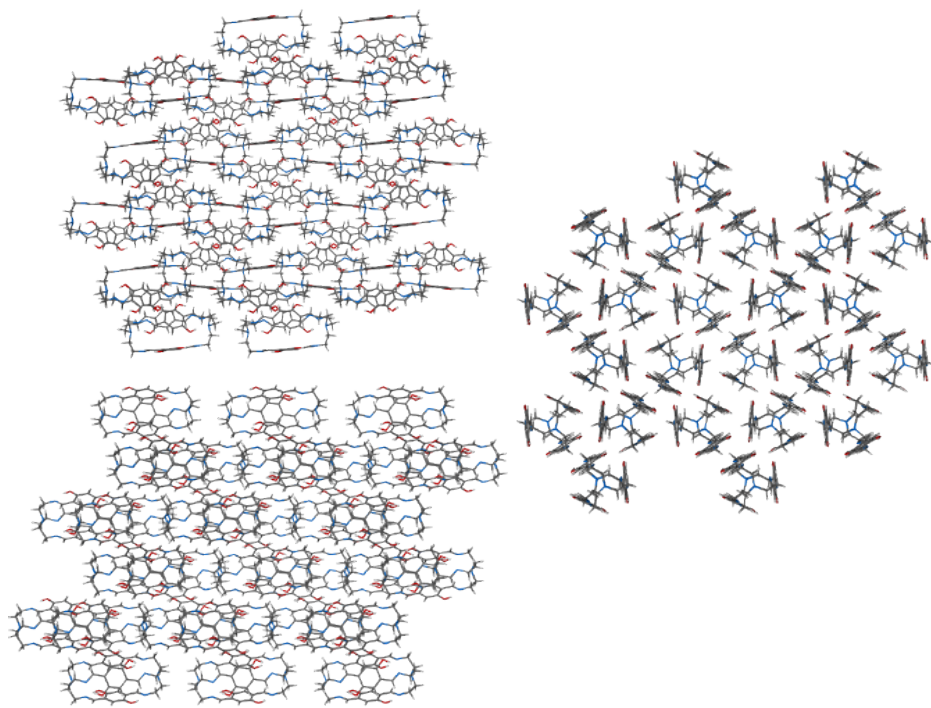


**Figure S18:** Crystal packing of **DIHO-cage@Py** when viewed along all the three crystallographic axes.

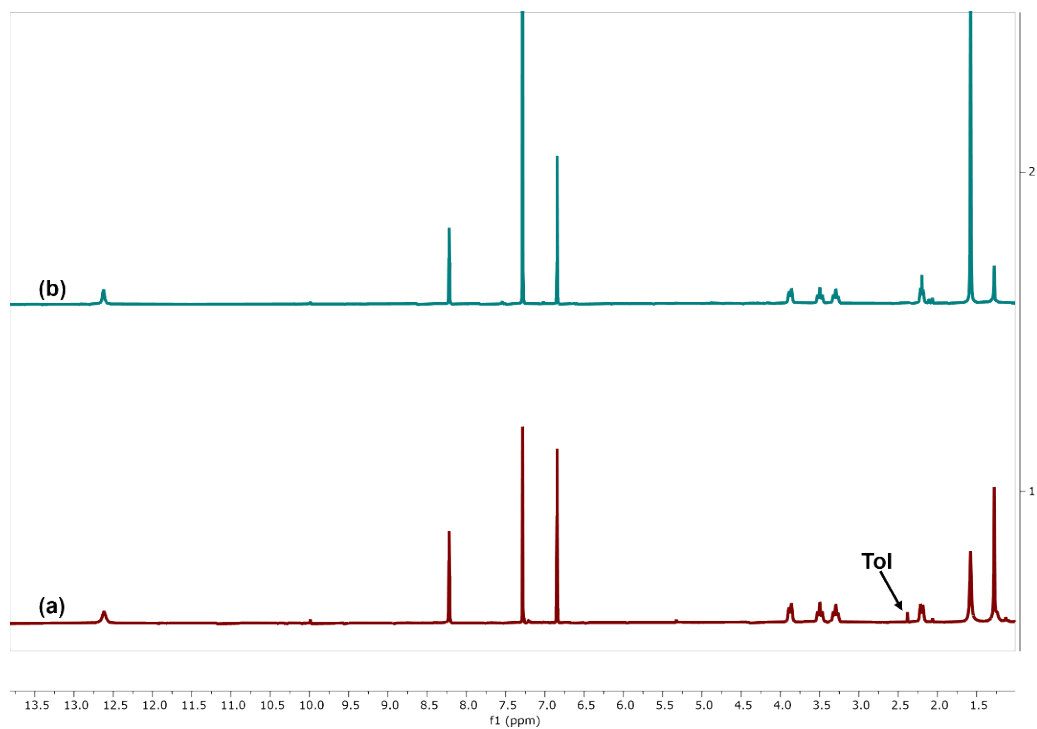


**Figure S19:** <sup>1</sup>H-NMR spectra (400 MHz, CDCl<sub>3</sub>, 293 K) showing (a) **DIHO-cage@Tol**; (b) Regenerated **DIHO-cage** after washing with n-hexane and heated at 45 °C under vacuum for 1 h.

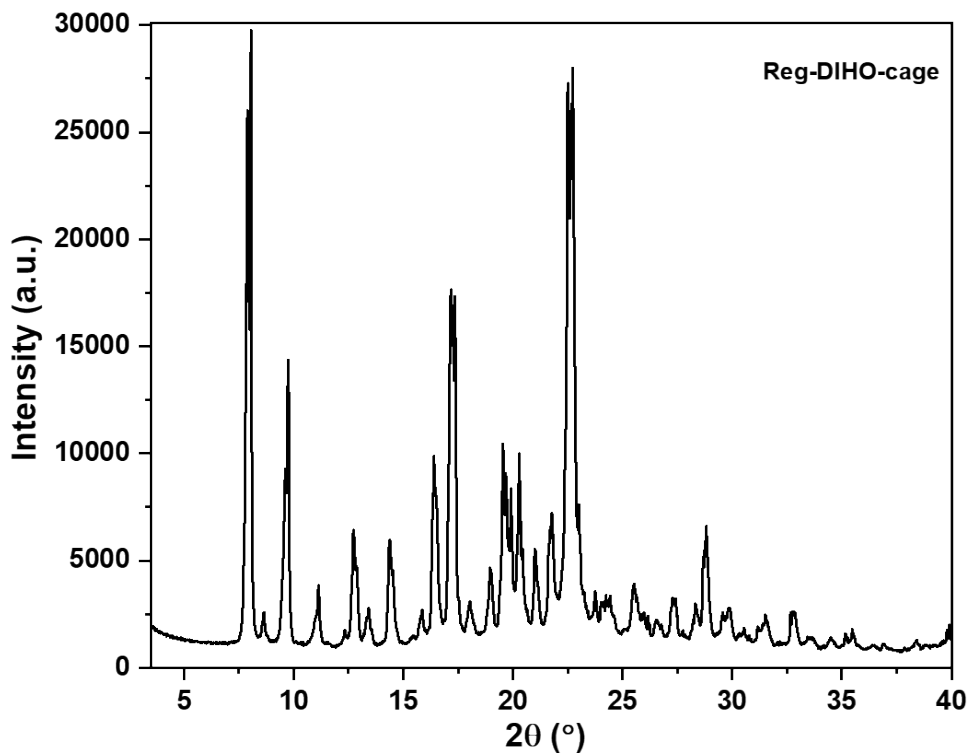


Figure S20: PXRD pattern of the regenerated DIHO-cage.

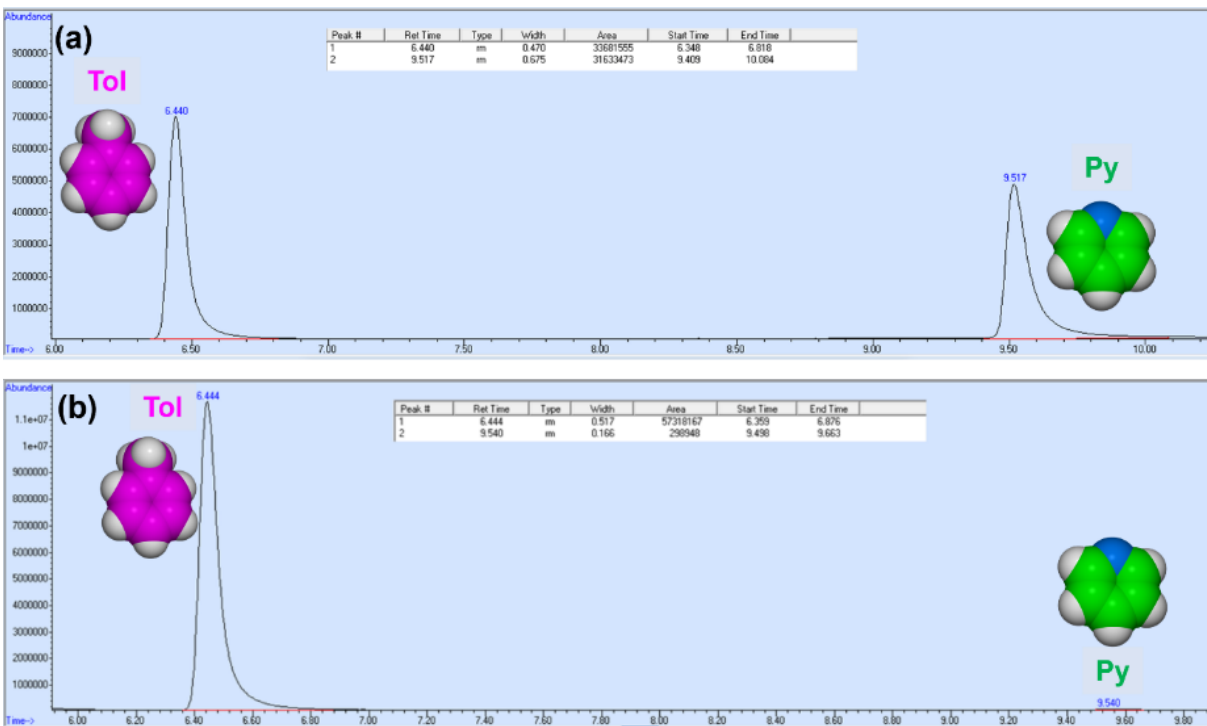


Figure S21: (a) Relative amount of Tol and Py in 1:1 (v/v) equimolar mixture of Tol/Py and (b) relative uptake of Tol and Py by DIHO-cage after adsorption as determined by gas chromatography.

**Table S1:** Crystallographic details of **DIHO-cage** in different solvents.

IDENTIFICATION CODE	DIHO-cage@CHCl <sub>3</sub>	DIHO-cage@DCM	DIHO-cage@Py	DIHO-cage@Tol	DIHO-cage@Tol/Py
Empirical formula	C <sub>38</sub> H <sub>44</sub> Cl <sub>6</sub> N <sub>8</sub> O <sub>6</sub>	C <sub>38</sub> H <sub>46</sub> Cl <sub>4</sub> N <sub>8</sub> O <sub>6</sub>	C <sub>36</sub> H <sub>42</sub> N <sub>8</sub> O <sub>6</sub>	C <sub>43</sub> H <sub>50</sub> N <sub>8</sub> O <sub>6</sub>	C <sub>43</sub> H <sub>50</sub> N <sub>8</sub> O <sub>6</sub>
Formula weight (g/mol)	921	852.63	682.77	774.91	774.92
Temperature /K	120	120.0	150	120	120
Crystal system	Monoclinic	Monoclinic	Monoclinic	Monoclinic	Monoclinic
Space group	<i>C2/c</i>	<i>P2<sub>1</sub>/c</i>	<i>P2<sub>1</sub>/n</i>	<i>P2<sub>1</sub>/c</i>	<i>P2<sub>1</sub>/c</i>
<i>a</i> / Å	19.3748(3)	16.3524(5)	13.685(4)	13.658(3)	13.5377(7)
<i>b</i> / Å	14.5735(2)	14.3350(4)	16.419(4)	9.8012(18)	9.7771(5)
<i>c</i> / Å	16.4860(2)	18.8597(5)	15.856(4)	30.782(5)	30.4812(15)
$\alpha$ /°	90	90	90	90	90
$\beta$ /°	115.7580(10)	113.765(2)	102.268(8)	99.251(12)	99.479(2)
$\gamma$ /°	90	90	90	90	90
Volume/ Å <sup>3</sup>	4192.43(11)	4046.1(2)	3481.4(16)	4067.0(13)	3979.4(3)
<i>Z</i>	4	4	4	4	4
$\rho_{\text{calc}}/\text{cm}^3$	1.460	1.400	1.303	1.266	1.293
<i>F</i> (000)	1912	1784	1448	1648	1653
Crystal size/mm <sup>3</sup>	0.1 x 0.2 x 0.3	0.1 x 0.2 x 0.3	0.1 x 0.2 x 0.3	0.1 x 0.2 x 0.3	0.1 x 0.2 x 0.3
Radiation	CuK $\alpha$ ( $\lambda$ = 1.54178)	CuK $\alpha$ ( $\lambda$ = 1.54178)	GaK $\alpha$ ( $\lambda$ = 1.34139)	CuK $\alpha$ ( $\lambda$ = 1.54178)	CuK $\alpha$ ( $\lambda$ = 1.54178)
reflections collected	29392	82129	85187	36177	72943
Independent reflections	3687( <i>R</i> <sub>int</sub> = 0.0651)	7412( <i>R</i> <sub>int</sub> = 0.0674)	8602 ( <i>R</i> <sub>int</sub> = 0.0838)	6639( <i>R</i> <sub>int</sub> = 0.0905)	7014( <i>R</i> <sub>int</sub> = 0.0428)
Data/restraints/parameters	2965/0/274	5864/0/529	7370/0/475	3527/0/522	7014/0/539
Goodness-of-fit on <i>F</i> <sup>2</sup>	1.024	0.982	1.076	0.997	1.059
Final <i>R</i> indexes [ <i>I</i> > 2 $\sigma$ ( <i>I</i> )]	<i>R</i> 1 = 0.0406, <i>wR</i> 2 = 0.1014	<i>R</i> 1 = 0.0511, <i>wR</i> 2 = 0.1411	<i>R</i> 1 = 0.0447, <i>wR</i> 2 = 0.1212	<i>R</i> 1 = 0.0547, <i>wR</i> 2 = 0.1395	<i>R</i> 1 = 0.0343, <i>wR</i> 2 = 0.0860
CCDC	2361427	2361428	2361429	2361430	2361431



**Table S2:** Some important host/guest hydrogen bonding intermolecular interactions between DIHO-cage and Tol in DIHO-cage@Tol crystal structure.

Distance	D...A (Å)	H...A (Å)	>D-H...A (°)
C11-H11B...i1	3.703	2.799	152.25
C25-H25A...i1	3.882	2.904	169.89
C39-H39...O5	3.434	2.810	124.10
C40-H40...O2	3.767	2.860	160.15
C41-H41...O4	3.756	3.043	133.03
C43-H43C...O3	3.497	2.566	158.48

**Table S3:** Some important host/host hydrogen bonding intermolecular interactions between DIHO-cages in DIHO-cage@Tol crystal structure.

Distance	D...A (Å)	H...A (Å)	>D-H...A (°)
C14-H14...O3	3.397	2.487	160.41
C22-H22...O1	3.383	2.441	171.29
C56-H56...N2	3.487	3.074	107.98

## References

1. Z. Cai, J. Du, T. Huang, Y. Ding and M. Wu, *CrystEngComm*, 2023, **25**, 5778–5781.
2. SAINT. Bruker AXS. Inc, Madison, Wisconsin, USA, 2014.
3. G. M. Sheldrick, SADABS. University of Gottingen, Germany, 2008.
4. G. M. Sheldrick, *Acta Crystallogr.*, 2008, **A64**, 112–122.
5. L. J. Barbour, *Supramol. Chem.* 2001, **1**, 189–191.
6. O. V. Dolomanov, L. J. Bourhis, R. J. Gildea, J. A. K. Howard and H. Puschmann, *J. Appl. Crystallogr.*, 2009, **42**, 339–341.